Single Ion Occupancy and Steady-state Gating of Na Channels in Squid Giant Axon

Robert F. Rakowski, David C. Gadsby, and Paul De Weer

Marine Biological Laboratory, Woods Hole, Massachusetts 02543

ABSTRACT The properties of the small fraction of tetrodotoxin (TTX)-sensitive Na channels that remain open in the steady state were studied in internally dialyzed voltage clamped squid giant axons. The observed Ussing flux ratio exponent (n') of 0.97 ± 0.03 (calculated from simultaneous measurements of TTX-sensitive current and ^{22}Na efflux) and nonindependent behavior of Na current at high internal [Na] are explained by a one-site ("*1s*") permeation model characterized by a single effective binding site within the channel pore in equilibrium with internal Na ions (apparent equilibrium dissociation constant $K_{Nai}(0) = 0.61 \pm 0.08$ M). Steady-state open probability of the TTX-sensitive channels can be modeled by the product $p_a p_\infty$, where p_a represents voltage-dependent activation described by a Boltzmann distribution with midpoint $V_a = -7$ mV and effective valence $z_a = 3.2$ (Vandenberg, C.A., and F. Bezanilla. 1991. *Biophys. J.* 60:1499–1510) coupled to voltage-independent inactivation by an equilibrium constant (Bezanilla, F., and C.M. Armstrong. 1977. *J. Gen. Physiol.* 70:549–566) $K_{eq} = 770$. The factor p_∞ represents voltage-dependent inactivation with empirical midpoint $V_\infty = -83 \pm 5$ mV and effective valence $z_\infty = 0.55 \pm 0.03$. The composite $p_a p_\infty$ *1s* model describes the steady-state voltage dependence of the persistent TTX-sensitive current well.

KEY WORDS: inactivation • tetrodotoxin • nonindependence • flux ratio • open probability

INTRODUCTION

In response to step depolarization, current through voltage-gated Na channels increases rapidly and then declines. The classical description of this gating behavior (Hodgkin and Huxley, 1952b,c) postulated two independent underlying processes, "activation" and "inactivation." Much work during the ensuing half-century has focused on these rapid (millisecond) gating events that underlie the generation and propagation of action potentials, and on the mechanisms of open channel permeation. The understanding gained has informed the study of other voltage-gated channels important in excitable cell function (Hille, 1992). Several early studies suggested the possibility of a second type of Na-channel conductance at positive membrane potentials (Adelman and Palti, 1969; Chandler and Meves, 1970; Bezanilla and Armstrong, 1977). Others demonstrated "slow" inactivation of the Na channel (Rudy, 1978; Almers et al., 1983; Kirsch and Anderson, 1986; Simoncini and Stühmer, 1987; Ruben et al., 1992). The existence of an alternative open Na-channel state arising from the inactivated state was established by Correa and Bezanilla (1994a,b) using macroscopic, gating, and single-channel current measurements. The importance for nerve function of such slower gating processes and of the very small persistent Na-channel current is now widely recognized (Crill, 1996; Cummins and Sigworth, 1996). Indeed, anticonvulsant and post-ischemia protective effects of drugs like lidocaine, carbamazepine, and phenytoin (for review see Taylor, 1993) may reflect their reduction of sustained Na-channel current.

The purpose of our experiments was twofold. First, we investigated the permeation properties of tetrodotoxin (TTX)*-sensitive Na channels that remain open in the steady state, exploiting a sensitive and stable voltage clamp in combination with isotopic flux measurements (Rakowski, 1989; Rakowski, Gadsby and De Weer, 1989). We determined the persistent Na current as the change in holding current caused by a saturating concentration of TTX. The concurrently measured change in ^{22}Na efflux allowed computation of both unidirectional fluxes and, hence, the Ussing flux ratio exponent (n'). Measurements of n' for K ion channels (Hodgkin and Keynes, 1955) provided strong evidence for a multi-ion (about three) pore that was recently confirmed by crystallography (Doyle et al., 1998; Morais-Cabral et al., 2001). Because Na channels undergo extensive inactivation both fast and slow, comparable data for these channels have been difficult to obtain. Our method offers the requisite stability and resolution, and our findings suggest occupancy of the Na-channel pore by, on average, a single Na ion.

Dr. Gadsby's present address is Laboratory of Cardiac/Membrane Physiology, Rockefeller University, 1230 York Avenue, New York, NY 10021. Dr. De Weer's present address is Department of Physiology, University of Pennsylvania, School of Medicine, 3700 Hamilton Walk, Philadelphia, PA 19104.

Address correspondence to Dr. R.F. Rakowski, Department of Biological Sciences, Ohio University, Irvine Hall, Athens, OH 45701. Fax: (740) 593-0300; E-mail: rakowski@ohio.edu

*Abbreviations used in this paper: P_o, open probability; TTX, tetrodotoxin.

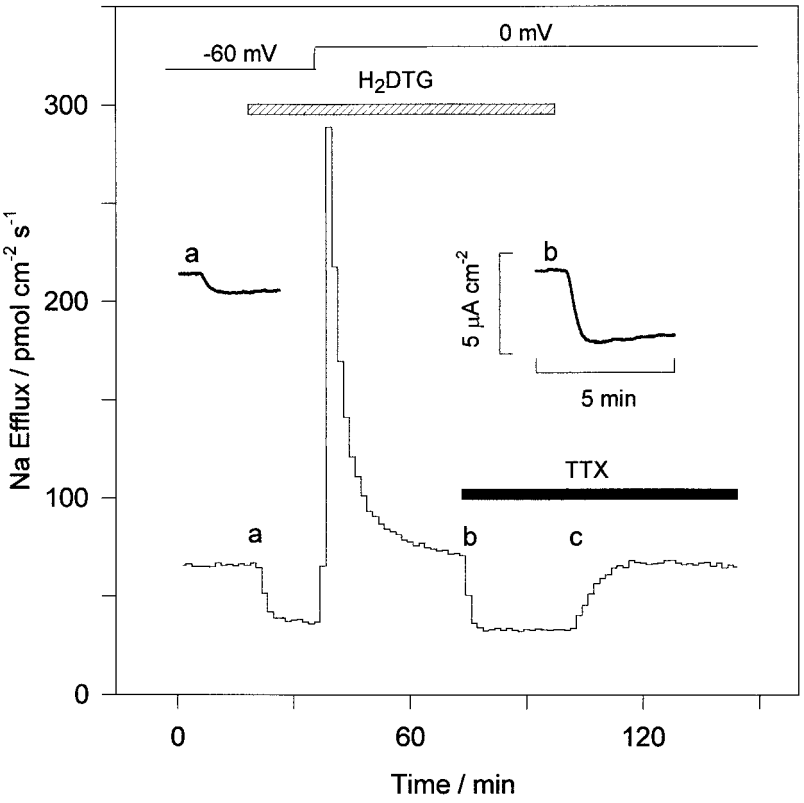

FIGURE 1. Equality of TTX-sensitive ^{22}Na efflux and current in Na-free extracellular solution. An axon internally dialyzed with 50 mM Na and 0.25 mM veratridine and superfused with Na-free, 10-mM K solution was clamped initially at −60 mV. (a) Addition of 10 μM dihydrodigitoxigenin (H_2DTG, a specific Na/K pump blocker) caused Na efflux to decrease by 34.6 pmol cm^{-2} s^{-1} and outward current by 1.0 μA cm^{-2}, which yields a pump-mediated Na efflux-to-current ratio of 3.3, which is compatible with the value of 3.0 expected for a 3 Na/2 K stoichiometry (Rakowski et al., 1989). Changing the holding potential to 0 mV in the continued presence of H_2DTG (and internal veratridine) elicited a large Na efflux, which then declined exponentially with a time constant of 4.00 ± 0.11 min. (b) Addition of 0.2 μM TTX caused Na efflux to decrease by 38.5 pmol cm^{-2} s^{-1} and outward current by 3.68 μA cm^{-2}, yielding a TTX-sensitive Na efflux-to-current ($F\Delta\Phi_{out}/\Delta I$) ratio of 1.01. (c) Washout of H_2DTG allowed recovery of 34.1 pmol cm^{-2} s^{-1} of Na/K pump-mediated Na efflux.

Our second objective was to analyze the voltage dependence of the open probability (gating) of the few Na channels that remain open in the steady state. The product $m^3(\infty)h(\infty)$ of the Hodgkin-Huxley (Hodgkin and Huxley, 1952c) analysis, which predicts the steady-state population of open Na channels of squid axon in the absence of slow inactivation, peaks at −47 mV with 0.5% of Na channels open. Incorporating steady-state "slow" inactivation (Rudy, 1978) yields the product $m^3(\infty)h(\infty)s(\infty)$, which peaks at −51 mV with 0.4% of Na channels remaining open. We find that neither model accurately predicts steady-state open probability or its voltage dependence. A simple alternative model that combines voltage-independent inactivation coupled to activation (Bezanilla and Armstrong, 1977) with an empirical Boltzmann equation encompassing all other voltage-dependent inactivation processes adequately accounts for our findings.

MATERIALS AND METHODS

Measurement of TTX-sensitive Current and Flux

TTX-sensitive current and ^{22}Na efflux were measured simultaneously in squid (*Loligo pealei*) giant axons as described previously (Rakowski, 1989; Rakowski et al., 1989). In brief, a 23-mm-long segment of squid giant axon cannulated at both ends was internally dialyzed via a cellulose acetate capillary made porous to low molecular weight solutes. A blackened platinum wire for passing current and a glass capillary electrode filled with 3 M KCl were inserted into the axon. The membrane potential was measured as the voltage difference between this internal electrode and an external flowing 3-M KCl reference electrode (to minimize junction potentials) placed near the solution outflow. A stable, low noise voltage clamp (Rakowski, 1989) controlled the membrane potential. The superfusion chamber, kept at 17–18°C, comprised two lateral pools that contained the cannulated axon ends, physically separated by grease seals from the central, superfused, experimental pool. Two ancillary voltage-clamp circuits kept the end and central pools at the same potential to prevent current flow between them. Efflux of ^{22}Na across the axon membrane in the experimental region was measured by collecting the central pool superfusate for later assay by either liquid scintillation or gamma counting. Data are presented as mean ± SEM. Log-normal statistics are applied to ratios.

Solutions

Internal and external solutions were the same as in Rakowski et al. (1989). The standard artificial seawater contained the following (in mM): 425 NaCl, 10 $CaCl_2$, 25 $MgCl_2$, 25 $MgSO_4$, 0.05 EDTA, and 5 Tris-HEPES, pH 7.7. 0.2 μM TTX was added from a 1-mM aqueous stock solution. In Na-free artificial seawaters, 425 mM NMG, TMA, or choline replaced Na; intermediate external Na concentrations were obtained by mixing. The high [Na] dialysate contained the following (in mM): 12.5 $MgSO_4$, 5 MgEGTA, 5 Na_2ATP, and 190 NaOH, pH 7.4 with ~500 mM HEPES. The osmolality of the dialysate was adjusted to within 1% of that of the extracellular solution (typically 940 mOsm kg^{-1}). In Na-free dialysate, 10 Tris and 190 NMG replaced Na. Intermediate internal Na concentrations also were achieved by mixing. In experiments to assess the inertness of internal NMG, it was replaced by equimolar TMA. In some early experiments, the internal solution also contained 5 mM potassium phosphoarginine.

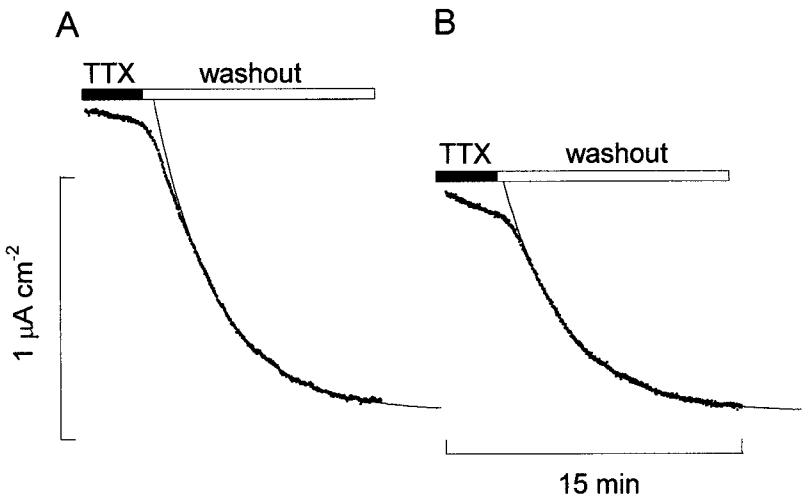

FIGURE 2. Recovery of inward current after removal of TTX. Axons were bathed in 425 mM Na seawater containing 0.2 μM TTX and internally dialyzed with 50 mM Na. Shortly after the bathing solution was replaced by one lacking TTX, the recovery of inward current became monoexponential. (A) Axon held at 0 mV. (B) A second axon held at −10 mV. Least-squares fits to the latter part of records A and B yielded exponential time constants of 3.19 ± 0.01 and 3.19 ± 0.02, respectively.

RESULTS

Our experimental approach demanded certain conditions: (1) membrane current and isotopic flux must be measured simultaneously from the same area of cell surface; (2) such measurements must be repeatable, reproducibly, on a preparation that has reached true steady state; (3) any spontaneous drift or channel rundown must be carefully monitored and corrected for; (4) inert nonpermeant Na replacements must be available; and (5) membrane potential must be measured accurately. We address each of these conditions before turning to the permeation properties and open probability of TTX-sensitive Na channels open in the steady state.

Simultaneous TTX-sensitive Current and Flux Measurements

Simultaneous measurement of TTX-sensitive current (ΔI) and ^{22}Na efflux ($\Delta\Phi_{out}$) is illustrated in Fig. 1, which also emphasizes the need to allow sufficient time to achieve steady state after membrane potential shifts. To enhance TTX-sensitive current in this experiment, the 50-mM Na internal dialysate contained 250 μM veratridine (Ohta et al., 1973). The current traces (Fig. 1, insets, a and b) have been scaled by Faraday's constant

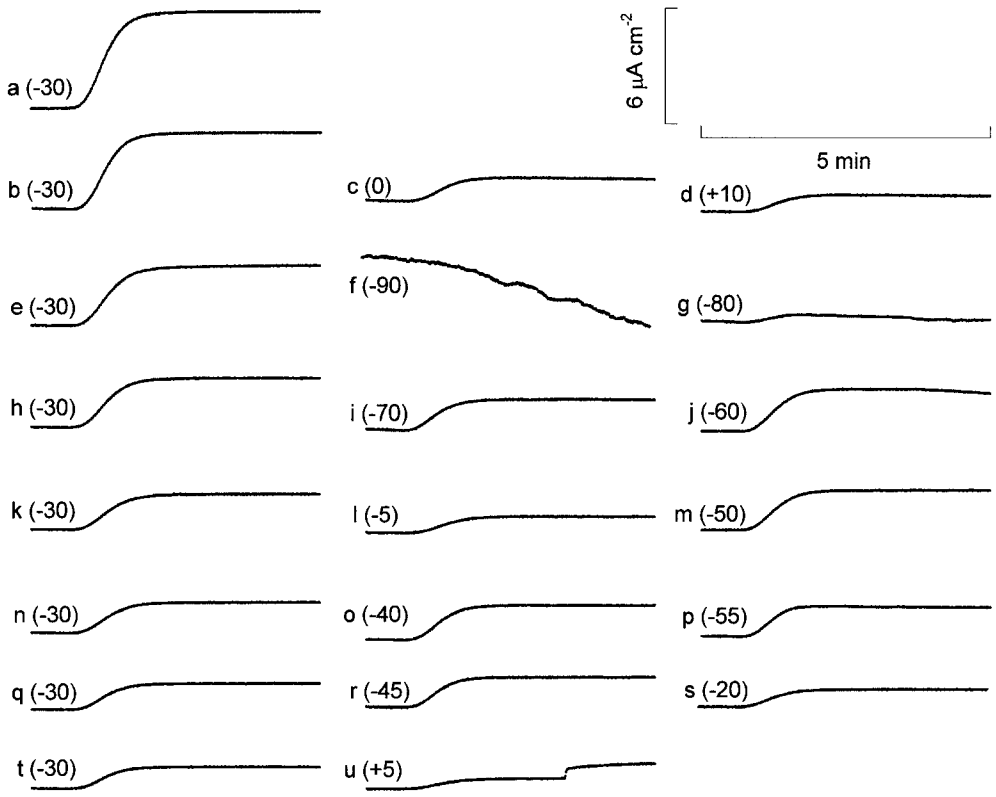

FIGURE 3. Repeated (in alphabetical order) exposures to 0.2 μM TTX (each followed by ~20 min of washout; not shown) of a single axon, bathed in 425 mM Na solution and internally dialyzed with Na-free solution, at various holding potentials. TTX reached the axon ~40 s into each 5-min record. The leftmost column shows all the records made at −30 mV.

to allow comparison of the amplitudes of changes in current (in μA cm^{-2}) and flux (in pmol cm^{-2} s^{-1}) which, on addition of TTX (Fig. 1 b), were similar. Our previous simultaneous measurements of TTX-sensitive Na efflux and outward current under the same zero-trans conditions (Na-free external solution) gave a mean flux/current ratio ($F\Delta\Phi_{out}/\Delta I$) of 1.00 ± 0.04 (Rakowski et al., 1989), which demonstrates that TTX-sensitive current and ^{22}Na efflux both derive from the same membrane area. A similar ratio, 1.05 ± 0.11, was obtained in five axons not exposed to veratridine (see Fig. 8). Veratridine was omitted in all subsequent experiments presented here.

Since many of our experiments required repeated exposure to TTX, it was important to establish the rate of recovery from block by TTX. In both axons of Fig. 2, the time constant for the exponential part of the recovery was 3.2 min. Since essentially complete recovery from TTX is achieved within 20 min, this was the minimum time allowed for TTX washout in all experiments.

Correction for Channel Rundown

Fig. 3 shows the outward shifts of holding current produced by 21 consecutive 5-min exposures of a single axon to TTX, at holding potentials between −90 and +10 mV. A semilog plot of all eight TTX-induced current shifts at −30 mV (Fig. 4 A, closed circles), which served as controls for rundown, shows a roughly exponential loss of functional TTX-sensitive channels with time. To estimate the initial magnitude of TTX-sensitive current that would have been measured at −30 mV without rundown, an exponential fit to the first three TTX-induced shifts under those reference conditions (425 mM external [Na], internal Na-free, −30 mV) was extrapolated to the start of dialysis (Fig. 4 A, closed triangle on the ordinate). Thus, the initial TTX-induced shift estimated for this axon was 5.7 ± 0.6 μA cm^{-2}, and the rundown time constant was 230 min. For 10 axons, the mean estimates were 3.3 ± 0.3 μA cm^{-2} and 340 ± 40 min, respectively; the cause of this rundown is unknown. The absolute magnitude of the holding current near the end of each exposure to TTX in the experiment of Fig. 3 is plotted against membrane potential in Fig. 4 B. The reproducibility of the repeated measurements at −30 mV over the 10-h period confirms the remarkable stability of the background current, in contrast to the TTX-sensitive current.

To correct TTX-induced current shifts recorded at other holding potentials (Fig. 3) for rundown, they must be scaled to the response predicted for −30 mV at the time of each measurement. These predictions (Fig. 4 A, open circles) were obtained by exponential interpolation (extrapolation for the final test) between successive measurements at −30 mV. TTX-sensitive currents normalized in this way for this axon are plotted against holding potential in Fig. 4 C. The theoretical curve shown was calculated using parameters obtained from a global least squares fit (see Table I in DISCUSSION) to all relevant data obtained in this work. The good agreement of this theoretical curve with the data in Fig. 4 C shows this one axon to be representative.

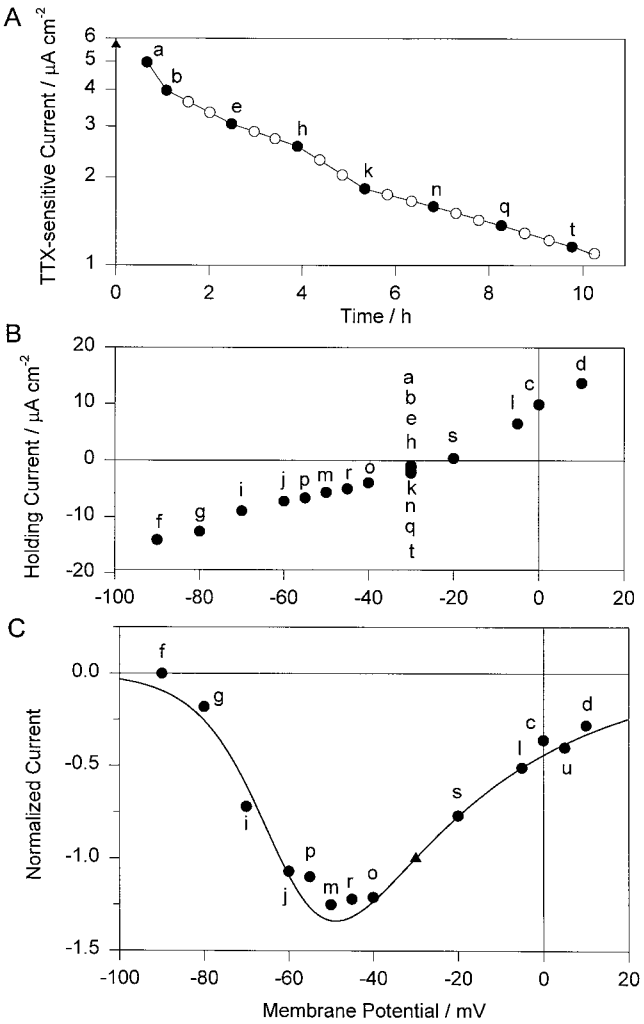

FIGURE 4. Steady-state TTX-sensitive and background currents at various membrane potentials. (A) TTX-sensitive currents measured at −30 mV in records a, b, e, h, k, n, q, and t of Fig. 3 are plotted (closed circles) on a semi-log scale against the time after starting dialysis. Estimated values for TTX-sensitive current at −30 mV at the start of dialysis (closed triangle on the ordinate) and at the times measurements were made at other holding potentials (open circles) were obtained as described in the text. (B) Steady-state background current, measured at various holding potentials in the presence of TTX, is plotted against membrane voltage. The eight measurements made at −30 mV over 9 h are almost superimposed. (C) TTX-sensitive currents recorded at various holding potentials in Fig. 3 c, d, f, g, i, j, l, m, o, p, r, s, and u were scaled (to correct for rundown) to the reference values at −30 mV (from A) and plotted against holding potential (closed circles). The closed triangle at −30 mV is the normalization point. The theoretical curve is described in the text.

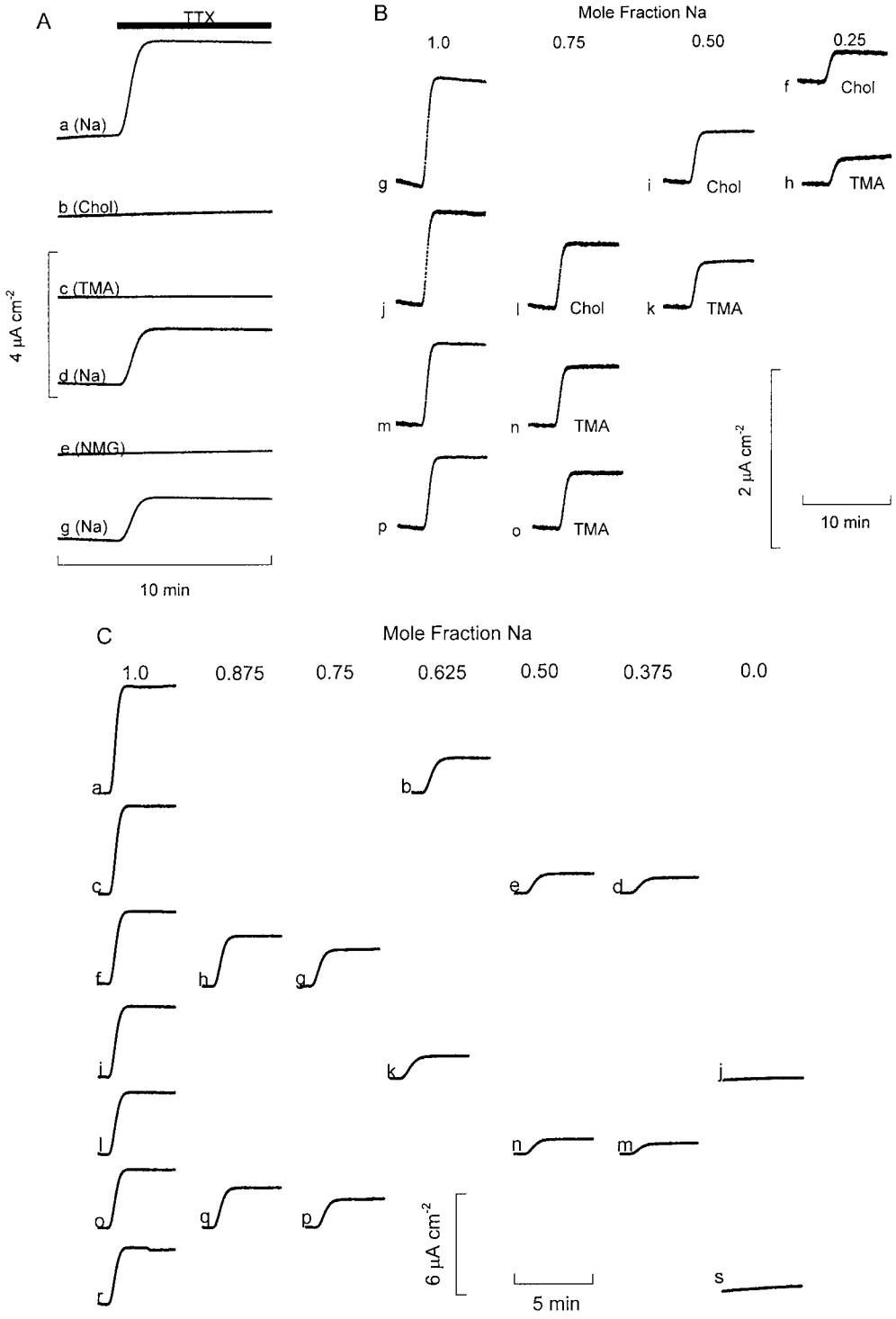

FIGURE 5. Full and partial replacement of external Na by NMG, choline, or TMA. Axons were held at −30 mV and internally dialyzed with Na-free solution. Records were taken in alphabetical order. (A) Repeated exposure to 0.2 μM TTX in 425 mM Na (a, d, and g), choline (b), TMA (c), or NMG (e). (B) Same axon as in A; experiment continued (f–p) to include partial replacement of external Na by choline or TMA. (C) Repeated exposure to 0.2 μM TTX in solutions with [Na] between 425 and 0 mM (see column headings for Na mole fraction) replaced by equimolar NMG.

NMG, Choline, and TMA Are Impermeant Substitutes for Na

Several experiments required inert substitutes for Na. No steady-state TTX-sensitive current was detected (Fig. 5 A) when NMG replaced all internal Na, and 425 mM choline (Fig. 5 A, b), TMA (Fig. 5 A, c), or NMG (Fig. 5 A, e) replaced all external Na (Fig. 5 A, a, d, and g), which signifies that all three cation substitutes are impermeant. Fig. 5 B shows records when external Na was only partially replaced by choline or TMA. At 0.5 mole fraction external Na (Fig. 5 B, i and k) the TTX-sensitive current was about half that seen in the nearest test with 425 mM Na (mole fraction 1.0), which suggests that TMA and choline are not only impermeant, but also inert, i.e., do not hinder Na permeation. In contrast to these findings with choline or TMA, partial replacement of exter-

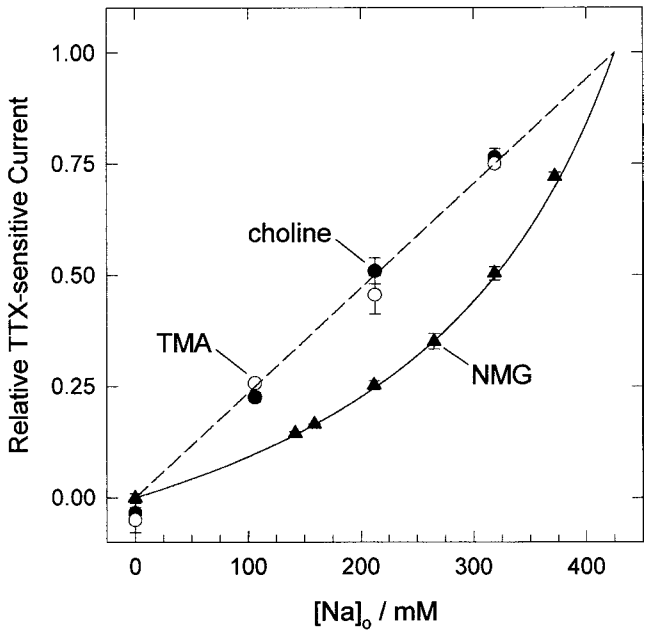

FIGURE 6. Summary of external-Na substitution experiments like those shown in Fig. 5. Relative TTX-sensitive inward current is plotted against external [Na]. Replacement for Na was either choline (closed circles; 7 axons), TMA (open circles; 7 axons), or NMG (closed triangles; 10 axons). SEM not shown when smaller than the symbol. The dashed and solid lines are drawn according to Eqs. 1 and 2, respectively.

nal Na by NMG (Fig. 5 C) reduced TTX-sensitive current further than expected if NMG were inert. For example, the size of the TTX-sensitive current at 0.5 mole fraction Na (Fig. 5 C, e and n) was about one quarter, rather than the anticipated one half, of that of the bracketing determinations at 425 mM Na. Average normalized data from 17 axons in which TMA, choline, or NMG replaced external Na are summarized in Fig. 6. With choline or TMA as substitutes, TTX-sensitive current was proportional to external Na concentration (Fig. 6, dashed line) as if the channel's apparent affinity for external Na were very low:

$$I_{Na}^{Rel} = \frac{[Na]}{425}, \qquad (1)$$

where [Na] is in mM. It can be shown that a linear relationship between current and the concentration of Na replacing another ion also would obtain if that ion were a competitive blocker, and if its apparent affinity were identical to that for Na. But the likelihood of TMA and choline sharing this special property must be small, and so we conclude that, instead, external TMA and choline are impermeant, nonblocking, substitutes for external Na and that the linear relationship (up to at least 425 mM Na_o) reflects a very low apparent affinity for external Na.

The curved line fitted to the NMG substitution data (Fig. 6) reflects a model in which external NMG binds to a site that, when occupied, blocks the channel:

$$I_{Na}^{Rel} = \frac{[Na]}{425} \cdot \frac{K_{NMG}}{K_{NMG} + [NMG]}, \qquad (2)$$

where K_{NMG} is the dissociation constant for NMG at that site. The low affinity for external Na precludes experimental distinction between competitive and noncompetitive inhibition by NMG. Nevertheless, other data discussed below suggest that the NMG binding site, unlike that for Na, lies at the external mouth of the channel outside the membrane electrical field. The overall least- squares fit (which also includes data from Fig. 10 A to be discussed below) gave an estimate for K_{NMG} of 209 ± 15 mM (see Table I). A similar inhibitory effect of external NMG was seen on ^{22}Na efflux (experiments not shown). Because NMG was our standard replacement for internal Na, we checked for block of outward TTX-sensitive current by internal NMG. TTX-sensitive outward current, measured at −45 mV in Na-free (choline) external solutions with a dialysate containing 105 mM Na and 105 mM of either NMG or TMA, averaged −0.046 ± 0.008 (n = 3) and −0.049 ± 0.006 (n = 2) μA cm^{-2}, respectively. On the assumption that internal TMA is an inert substitute for internal Na (but see Horn et al., 1981), as established above for external TMA, this result implies that internal NMG does not inhibit TTX-sensitive channels. The alternative possibility is rendered unlikely by the close agreement between the currents measured with NMG or TMA, which would require the apparent K_i for any putative block by internal NMG and TMA at −45 mV to be identical.

We also examined whether small amounts of contaminating internal K, or the 5-mM internal K added as potassium phosphoarginine in early experiments, support a detectable outward TTX-sensitive current. Although, with 200 mM Na in the dialysate, we observed the usual, substantial, TTX-sensitive outward current in Na-free (choline) external solution, after exchanging the dialysate for one containing 5 mM K, but no Na (replacement: NMG), we could detect no TTX-sensitive current in Na-free external solution containing either choline or TMA (two measurements on one axon). Thus, up to 5 mM contaminating internal K carries no measurable TTX-sensitive steady-state current even in the absence of competing internal or external Na.

Accuracy of Membrane Potential Measurement: Reversal of the TTX-sensitive Current

To observe both inward and outward steady-state TTX-sensitive currents in an axon under fixed ionic conditions, we chose appropriate Na concentrations (184 mM inside and 111 mM outside, confirmed by flame photometry). Fig. 7 A shows records of repeated exposures

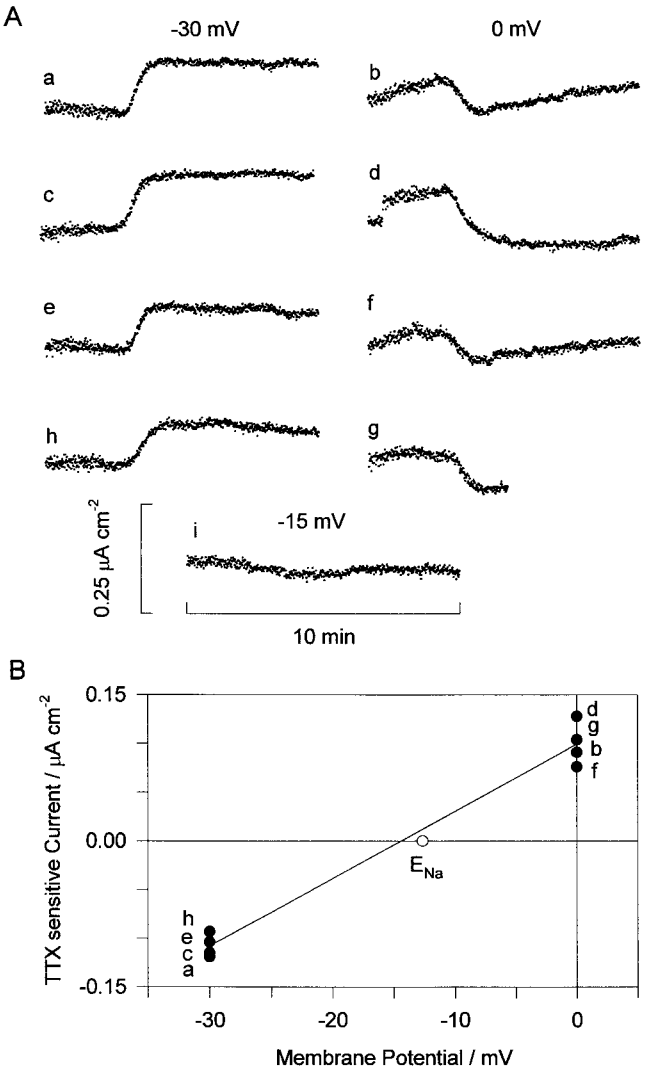

FIGURE 7. Reversal potential of the steady-state TTX-sensitive current. (A) An axon dialyzed with 184 mM Na and bathed in 111 mM Na (choline substitution) was repeatedly exposed to 0.2 μM TTX. Measurements were made at holding potentials of −30, 0, and −15 mV in the alphabetical sequence shown. (B) The TTX-sensitive current changes measured in A are plotted (closed circles) against the holding potential. The current change measured at −15 mV was not different from zero. The calculated equilibrium potential for Na (−12.7 mV) is shown as the open circle (E_{Na}). The solid line connecting the means at −30 and at 0 mV crosses the voltage axis at −14.4 mV.

to TTX alternately at −30 or 0 mV (Fig. 7 A, a–h), and at −15 mV (Fig. 7 A, i). The magnitudes of the TTX-sensitive currents (Fig. 7 B) gave (by linear interpolation) an estimate for the reversal potential of −14.4 mV, close to the calculated value of E_{Na} (−12.7 mV). A second axon treated similarly gave a reversal potential of −14.6 mV. These findings corroborate the accuracy of our membrane potential measurements (i.e., within 2 mV).

Flux Ratio Exponent

TTX-sensitive ^{22}Na efflux and net current were simultaneously measured (Fig. 8) in axons held at −30 mV, internally dialyzed with 200 mM Na, and exposed alternately to 425 mM external Na (b, d) or choline (a, c). Five axons in the Na-free solution gave mean values of 0.198 ± 0.009 μA cm^{-2} (n = 17 trials) for TTX-sensitive current and 2.15 ± 0.22 pmol cm^{-2} s^{-1} (n = 15 trials) for TTX-sensitive ^{22}Na efflux, yielding a ratio $F\Delta\Phi_{out}/\Delta I$ = 1.05 ± 0.11. This good agreement with the expected ratio of 1.0 and with our findings on veratridine-treated axons (Fig. 1) validates our comparisons of simultaneously measured flux and current. The magnitudes of TTX-induced changes in net current and unidirectional efflux in 425 mM external and 200 mM internal Na solution (Fig. 8, episodes b and d) can be used to calculate the Ussing flux ratio exponent (Ussing, 1949; Hodgkin and Keynes, 1955). Thus, the TTX-sensitive net current (ΔI) represents, via Faraday's constant, a net flux (ΔΦ) from which the simultaneously measured unidirectional ^{22}Na efflux component ($\Delta\Phi_{out}$) can be subtracted to yield unidirectional influx ($\Delta\Phi_{in}$). The flux ratio exponent (n') then follows from Eq. 3

$$\frac{\Delta\Phi_{out}}{\Delta\Phi_{in}} = \left(\frac{[Na]_i}{[Na]_o} \cdot e^{\frac{VF}{RT}}\right)^{n'}. \quad (3)$$

For eight paired measurements of ΔI and $\Delta\Phi_{out}$ on four axons at a holding potential (V) of −30 mV, we find n' = 0.97 ± 0.03. For visual corroboration of this result, we show in Fig. 8 C (smoother downward traces in b and d) the hypothetical TTX-induced current shift expected for abolition of the outward component alone, which is computed from the actually observed net current shift assuming a flux ratio exponent n' = 1.

Comparison of TTX-sensitive Currents with and without trans Na Present: Evidence for Nonindependence

According to the independence principle, "the chance that any individual ion will cross the membrane in a specified interval of time is independent of the other ions which are present" (Hodgkin and Huxley, 1952a). To test whether Na fluxes are influenced by Na present on the trans side, we measured TTX-sensitive currents first under zero-trans conditions, i.e., with Na present either on the outside of the axon only (Fig. 9, left column) or on the inside only (Fig. 9, middle column), and then with Na on both sides (Fig. 9, right column). The measurements were made in the (alphabetical) order shown, and all were subject to rundown, so that comparison required interpolation between adjacent pairs of like measurements. The traces marked by asterisks in the right column are hypothetical and were constructed as the sum of the two zero-trans currents (Fig. 9, left and middle columns), both interpolated to the time of the actual

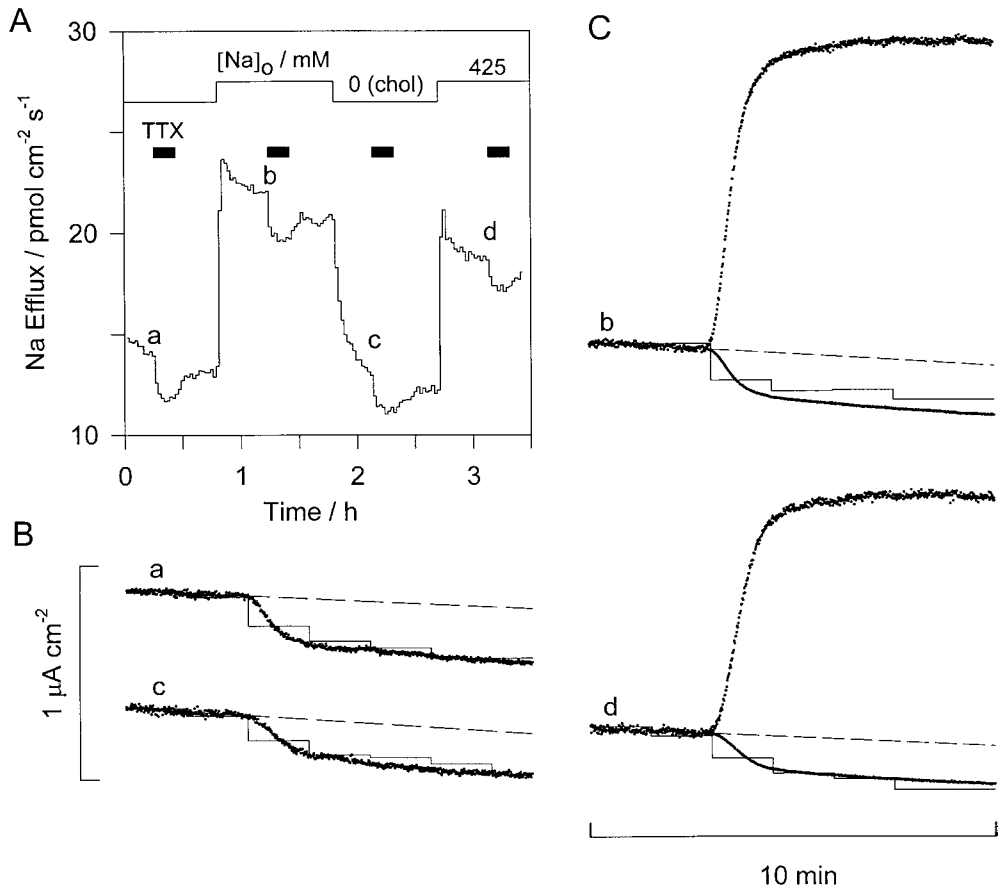

FIGURE 8. Determination of the flux ratio exponent n'. (A) An axon held at −30 mV and internally dialyzed with 200 mM radiolabeled Na was repeatedly exposed to 0.2 μM TTX in 425 mM choline, Na-free solution (a and c) or in 425 mM Na, choline-free solution (b and d). (B) The two TTX induced ^{22}Na efflux drops in Na-free (choline) solution (a and c) are replotted on expanded time bases and scaled by Faraday's constant, together with the TTX-induced shifts in holding current recorded at the same time. (C) Comparison of current transients b and d (also on expanded time bases) with the simultaneously measured drop in ^{22}Na efflux. TTX addition in the presence of 425 mM external Na blocked (net) inward currents (noisy traces; 1.47 and 1.11 μA cm^{-2}, respectively). For illustration, a theoretical outward component of the observed net current was computed assuming an Ussing flux ratio exponent $n' = 1$, and is shown (inverted) in each case as a smoother downward trace superimposed on the corresponding observed drop in ^{22}Na efflux.

measurement (Fig. 9, right column, no asterisk) with Na present on both sides. Evidently, the in- and outward movements of Na did not obey independence, as the net current measured with Na present on both sides (Fig. 9, right column) was significantly and consistently smaller than the sum of the corresponding zero-trans currents. The observed net current averaged 0.81 ± 0.01 (n = 7 on two axons) of the sum of the corresponding zero-trans currents. A measurement artifact is highly unlikely since (1) each comparison was made on a single axon at constant holding potential and only the solutions were varied; (2) liquid junction potentials at the external reference electrode were minimized by means of a flowing 3-M KCl junction; and (3) any liquid junction potential difference at the internal electrode between Na-containing and Na-free dialysates would be expected to exaggerate, not lessen, the discrepancy depicted in the right-hand column of Fig. 9.

Furthermore, the observed zero-trans TTX-sensitive outward current (inward shifts, middle column) is significantly (17%) smaller than calculated (assuming independence) for the same potential from the (appropriately interpolated) corresponding zero-trans inward current (outward shifts, left column): the observed ratio of zero-trans currents averaged −0.123 ± 0.003 (n = 12 from 2 axons) compared with −0.149 predicted at −30 mV for independent zero-trans fluxes at 425 mM external and at 200 mM internal [Na]. This observation furthers the evidence against independence. Although a sizeable constant error in our measurement of membrane potential (−35 mV instead of −30 mV) would be able to account for the discrepancy and, thus, weaken it as evidence, such a large error seems unlikely in view of the good agreement we find between computed and measured reversal potentials (Fig. 7). Moreover, this smaller-than-expected zero-trans outward Na current cannot be attributed to block by external choline, which we have shown (Figs. 5 and 6) to be an inert substitute for Na. Finally, any channel block by internal NMG, which was present only during the measurements of zero-trans inward Na current in these experiments (Fig. 9, left column, 425/0), could only cause us to underestimate the size of that inward current: in

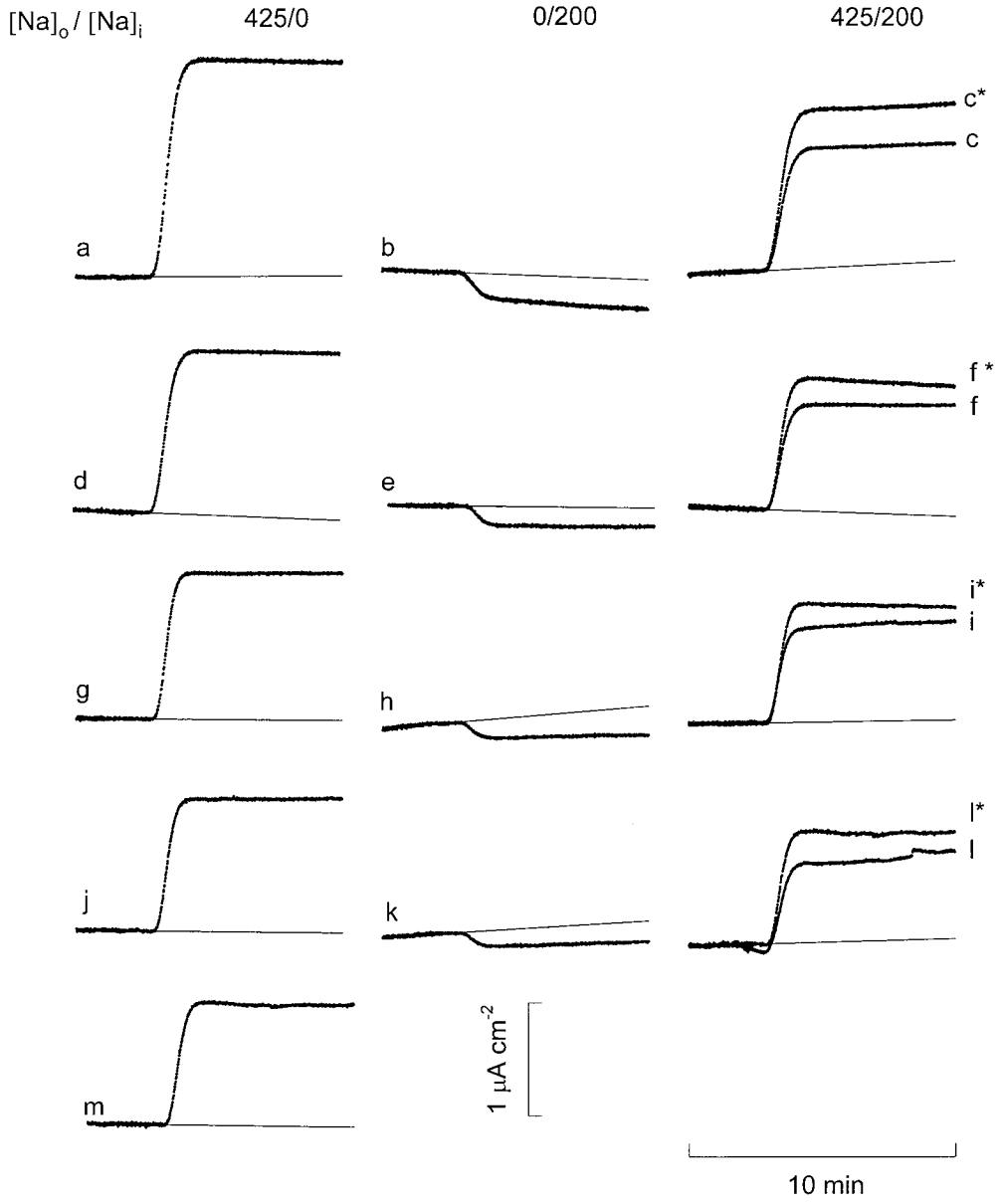

FIGURE 9. TTX-sensitive current with Na-free internal or external solution or with Na present on both sides. An axon held at −30 mV was initially dialyzed with Na-free (NMG) solution and bathed in 425 mM [Na]. After the response to 0.2 μM TTX was recorded (a), the dialysate was replaced by one containing 200 mM [Na] and the external medium by a Na-free, TTX-free solution (choline substitution). After another 30 min of dialysis, the response to 0.2 μM TTX was measured again (b). The external solution was then changed to TTX-free, 425 mM Na solution. After 30 min, the response to TTX was measured a third time (c). The record shown as c* was calculated from a, b, d, and e as described in the text. This protocol was repeated three more times in the same axon (records d–m), and a similar experiment with three repetitions of the protocol was done in another axon.

turn, this would cause us to also underestimate the degree of nonindependence.

Voltage Dependence of Steady-state TTX-sensitive Current

We have already illustrated (Figs. 3 and 4) our method for examining the voltage dependence of steady-state TTX-sensitive inward current in axons exposed to 425 mM Na and dialyzed with Na-free solution. We similarly examined the voltage dependence of outward persistent TTX-sensitive currents in axons dialyzed with 200 mM Na and exposed to Na-free (choline) solutions. To permit direct comparison of normalized outward currents with normalized inward currents, we exploited data from experiments like that in Fig. 9 in which both types of TTX-sensitive current were measured in a single axon at a constant holding potential of −30 mV. Two further conditions were also examined: (1) with 50 mM Na inside and 425 outside; and (2) with 266 mM Na plus 159 mM NMG outside and Na-free solution inside.

All of our data concerning the steady-state voltage dependence of TTX-sensitive currents obtained under these four experimental conditions, annotated as (external [Na]/internal [Na], both in mM) 425/0, 425/50, 266/0, or 0/200, are summarized in Fig. 10 A. The theoretical curves through the data represent the currents calculated for each of the four ionic conditions, using a single set of parameters obtained from a simultaneous least-squares fit to all relevant data of an economical steady-state gating and permeation model that postulates a single binding site for Na in the pore (the $p_a p_\infty 1s$ model, to be presented in the DISCUSSION). In the global least-squares fit, the estimation of individual model

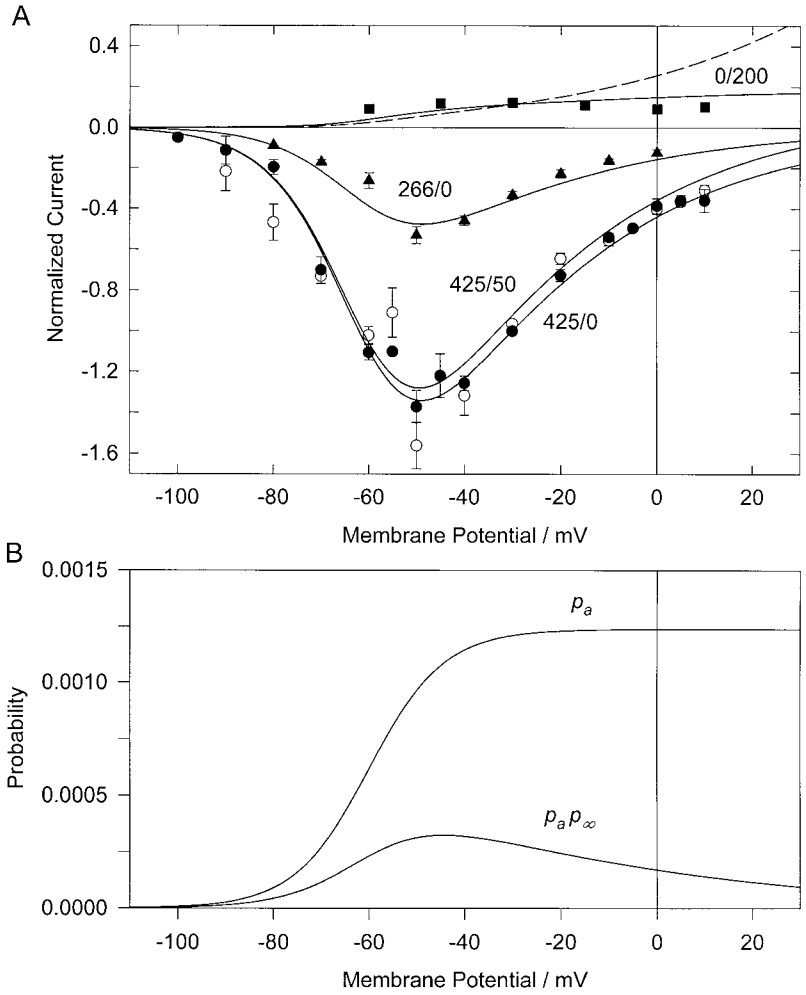

Figure 10. Summary of the steady-state voltage dependence of normalized TTX-sensitive currents. (A) TTX-sensitive currents were measured at the Na concentrations indicated, given (in mM) as external [Na]/internal [Na]: 425/0 (nine axons; closed circles); 425/50 (nine axons; open circles); 266 (NMG replacement)/0 (nine axons; closed triangles); and 0 (choline replacement)/200 (seven axons; closed squares). Current amplitudes under all four conditions, at each membrane potential, were normalized to the current at −30 mV with 425 mM external Na and zero internal Na. The solid lines are calculated from a least-squares fit, to the entire dataset, of a permeation, steady-state gating, and (for the 266/0 condition) NMG block model described in DISCUSSION. The dashed line is described in the text. (B) Theoretical steady-state channel open probability functions p_a (Eq. 10) and $p_a p_\infty$ (product of Eqs. 10 and 12), as described in DISCUSSION, calculated with the overall least-squares fit parameters listed in Table I.

parameters is governed by various data subsets: (1) the gating parameters are governed by the voltage dependence data (Fig. 10 A); (2) the apparent dissociation constant for binding of internal Na, K_{Nai}, by the ratios of current amplitudes at −30 mV in the 425/200 and 0/200 conditions to those in 425/0 (Fig. 9) as well as by the in- versus outward current pairs over a range of voltages (Fig. 10 A); and (3) the K_{NMG} for channel block by external NMG by data of Fig. 6 together with the 266/0 curve of Fig. 10 A. The assumption of voltage-independent block by external NMG is validated here by the demonstration that inward currents measured in the presence of 159 mM external NMG are adequately fit (266/0 curve; Fig. 10 A) by an equation that is scaled uniformly across the entire voltage range by a single factor appropriate for block by that concentration of NMG. The theoretical curves in Fig. 10 B will be described in the DISCUSSION. The dashed line in Fig. 10 A represents the outward current expected in 0/200 conditions for a model (Fig. 10 B, curve p_a) that lacks voltage-dependent inactivation (i.e., $p_a 1s$, without p_∞). Its poor fit to the 0/200 data demonstrates (see DISCUSSION) the need to include voltage-dependent inactivation (Fig. 10 B, curve $p_a p_\infty$) in our $p_a p_\infty 1s$ model.

DISCUSSION

The presumption seems justified that the extremely small fraction of TTX-sensitive channels that remain open in the steady state represent "classical" voltage-sensitive Na-selective channels: the experimental reversal potential of the currents they carry was close to the theoretical value for E_{Na}; choline, TMA, and NMG were impermeant; and recovery from TTX inhibition had a time course similar to that found for classical Na channels. Flux ratio measurements revealed an Ussing flux ratio exponent close to 1.0. However, inward and outward Na movements were not independent of one another, a property that requires at least one saturable, if low affinity, binding site for Na ions within the pore. Moreover, as discussed in the section on persistent gating, voltage dependence of channel open probability was consistent with literature values of the steady-state gating parameters that describe voltage-dependent activation and fast voltage-independent inactivation of Na

channels, but necessitated an additional parameter describing steady-state voltage-dependent inactivation.

Minimal Model for Nonindependent Sodium Permeation that Exhibits an Ussing Flux Ratio Exponent (n') of Unity

From eight paired measurements of TTX-sensitive current and ^{22}Na efflux including those in Fig. 8 with 425 mM external and 200 mM internal Na, we find an Ussing flux ratio exponent (n') of 0.97 ± 0.03. This removes the need to postulate a multi-ion pore to account for the ion flux behavior under our experimental conditions. A flux ratio exponent of unity implies ion movements that either obey the independence principle or are mediated by (effectively) one-site channels; multi-site channels with very low occupancy (rarely exceeding one ion per channel) also yield n' values close to one (Hille and Schwarz, 1978; Begenisich, 1987). However, Fig. 9 shows that ion movements through persistent Na channels are not independent, as net current measured with Na both inside (200 mM) and outside (425 mM) is less than the sum of the corresponding zero-trans currents. Nonindependence requires that permeating ions interact with, i.e., "bind" to a "site" within, the channel. Since the Ussing flux ratio exponent of unity does not require a multi-ion pore, this observed deviation from independence can be explained by a simple permeation model (Scheme I):

$$E + Na_o \underset{k_{-1}}{\overset{k_1}{\rightleftharpoons}} ENa \underset{k_{-2}}{\overset{k_2}{\rightleftharpoons}} E + Na_i$$

(SCHEME I)

in which both external Na (Na_o) and internal Na (Na_i) have direct access to a single effective binding site in the pore of the channel protein (E). This effective binding site could, in reality, be distributed over several physically distinct points in space as long as occupancy of the "site" precludes concomitant binding of a second ion in the pore. At this site, the permeating ion senses a fraction δ_{Na} (arbitrarily set here at 0.5) of the electrical field (from the internal solution), so that the rate coefficients $k_1 \ldots k_{-2}$ of Scheme I become functions $k_1(\mathrm{V}) \ldots k_{-2}(\mathrm{V})$ (defined in Eqs. 8 and 9) of membrane potential. In the absence of membrane potential ($V = 0$), microscopic reversibility constrains as follows:

$$\frac{k_1(0)}{k_{-1}(0)} = \frac{k_{-2}(0)}{k_2(0)}. \tag{4}$$

The expressions for zero-trans Na influx (inward flux is negative) and efflux rates (i.e., ions traversing each pore per unit time) are as follows:

$$\Phi_{in}^{zero\text{-}trans} = \frac{-k_1 k_2 [Na]_o}{k_{-1} + k_2 + k_1 [Na]_o} \quad \text{and}$$
$$\Phi_{out}^{zero\text{-}trans} = \frac{k_{-1} k_{-2} [Na]_i}{k_{-1} + k_2 + k_{-2} [Na]_i}. \tag{5}$$

Our finding that TTX-sensitive inward current is a linear function of external [Na] (Fig. 6) while a finite apparent affinity for internal Na is required to account for the observed nonindependence (Fig. 9) permits a further simplification. These features are satisfied over practical voltage ranges by setting the rate coefficients for transitions between binding site and internal solution, k_2 and k_{-2}, very large compared with those for the transition between binding site and external solution, k_1 and k_{-1}:

$$k_2, k_{-2} \gg k_1, k_{-1}.$$

Zero-trans influx (Eq. 5, top) will then be linearly proportional to $[\mathrm{Na}]_o$ as required by Fig. 6, whereas $K_{0.5}(\mathrm{Na}_i)$ (given by $(k_{-1} + k_2)/k_{-2}$ [Eq. 5, bottom]) assumes a finite value as required of the saturable binding site that underlies nonindependence. The simplification yields:

$$E + Na_o \underset{k_{-1}}{\overset{k_1}{\rightleftharpoons}} ENa \overset{K_{Nai}}{\longleftrightarrow} E + Na_i$$

(SCHEME II)

in which equilibrium prevails between binding site and internal solution, governed by the equilibrium dissociation constant for internal sodium binding, $K_{Nai}(\mathrm{V}) = k_2(\mathrm{V})/k_{-2}(\mathrm{V})$. The net flux is then:

$$\Phi_{net} = \frac{k_{-1}(V)[Na]_i - k_1(V) K_{Nai}(V)[Na]_o}{K_{Nai}(V) + [Na]_i}. \tag{6}$$

From Boltzmann's law the equilibrium constant varies with membrane voltage, decreasing with depolarization (steepness being determined by δ_{Na}) as given by Eq. 7:

$$K_{Nai}(V) = K_{Nai}(0) \cdot e^{\frac{(\delta_{Na} - 1)VF}{RT}}. \tag{7}$$

The sole determinants of site occupancy, therefore, are internal [Na] and membrane potential. For simplicity, we further assume symmetry in the effect of membrane potential on the rate coefficients k_1 and k_{-1}:

$$k_1(V) = k_1(0) \cdot e^{\frac{-\delta_{Na} VF}{2RT}} \tag{8}$$

$$k_{-1}(V) = k_{-1}(0) \cdot e^{\frac{\delta_{Na} VF}{2RT}}. \tag{9}$$

As our fluxes are normalized to a reference value, and because of Eq. 4, only a single adjustable parameter

(K_{Nai}) is required to account for the open-channel flux properties in the absence of NMG. The least-squares value for $K_{Nai}(0)$ (see Table I) yields a $K_{Nai}(V)$ of 1.12 M at −30 mV. From measurements of peak Na-channel current as a function of internal ion activity, Begenisich and Cahalan (1980a,b) found a K_{Nai} of 0.86 M at +25 mV. Our value for K_{Nai} at −30 mV correctly predicts the nonindependence of unidirectional fluxes we observed: net flux under 425/200 conditions is calculated to be only 0.82 of the sum of fluxes measured under the corresponding zero-trans conditions 425/0 and 0/200 (observed current ratio was 0.81 ± 0.01; Fig. 9). Furthermore, the model predicts a ratio of currents under zero-trans (0/200 and 425/0) conditions of −0.125, which is compatible with the observed current ratio of −0.123 ± 0.003.

The *1s* model has an obligatory Ussing flux ratio exponent of unity (we observed 0.97 ± 0.03). Begenisich and Busath (1981) also found a value (1.03 ± 0.04) not significantly different from 1, and independent of voltage between −22 and +33 mV. Though a one-site model suffices to account for these data, multi-site models that have low occupancy could also explain them, but need more parameters than can be uniquely determined. Such a multi-site (but single ion occupancy) model for the Na channel has been invoked to describe Na current-voltage relationships (Hille, 1975). Begenisich (1987) concluded that, although two sites are needed to explain the concentration dependence of the P_K/P_{Na} permeability ratio, both sites are rarely simultaneously filled. We conclude that the Na channel either has one effective binding site with relatively low affinity or is a multi-site channel rarely occupied by more than one Na ion at a time. It remains to be seen whether other models of ion permeation such as the Poisson-Nernst-Planck formulation (Nonner et al., 1998; Levitt, 1999) can also explain the observed deviations from independence.

Gating Model for the Persistent Na Channels

Three processes govern the theoretical curves in Figs. 4 and 10 A: channel gating, open channel permeation, and (for the data at 266 mM external [Na]) block by external NMG. Our least-squares fit to the data uses two independent (i.e., multiplicative) factors for steady-state channel gating: one (p_a) reflecting activation coupled to voltage independent inactivation, and a second (p_∞) encompassing all other (voltage dependent) inactivation processes. The first factor (p_a) is the steady-state open probability function for Scheme III:

$$C \rightleftarrows O \rightleftarrows I \qquad \text{(SCHEME III)}$$

in which activation and voltage-independent inactivation are coupled (Goldman and Schauf, 1972; Bezanilla and Armstrong, 1977) rather than independent:

$$p_a = \frac{a(\infty)}{1 + a(\infty)K_{eq}}, \tag{10}$$

where $a(\infty)$ describes the steady-state voltage dependence of channel activation ($C \rightleftarrows O$), and K_{eq} is a voltage-independent equilibrium constant governing inactivation ($O \rightleftarrows I$). For the steady-state activation function, $a(\infty)$ we use a Boltzmann distribution

$$a(\infty) = \frac{1}{1 + e^{\frac{z_a(V_a - V)F}{RT}}}, \tag{11}$$

with midpoint $V_a = -7$ mV and effective valence $z_a = 3.2$, as determined by Vandenberg and Bezanilla (1991) in *L. pealei* axons under ionic conditions comparable to ours. For the voltage-dependent steady-state inactivation factor (p_∞), a Boltzmann distribution function

$$p_\infty = \frac{1}{1 + e^{\frac{z_\infty(V - V_\infty)F}{RT}}}, \tag{12}$$

with empirical midpoint $V_\infty = -83$ mV and effective valence $z_\infty = 0.55$ was found to be sufficient. The five parameters (K_{eq}, z_a, V_a, z_∞, and V_∞) that describe the channel's open probability (Eqs. 10–12) are constrained by the experimental open probability

$$P_o = \frac{1}{\left[K_{eq} + 1 + e^{\frac{z_a(V_a - V)F}{RT}}\right] \cdot \left[1 + e^{\frac{z_\infty(V - V_\infty)F}{RT}}\right]} \tag{13}$$

for which we have an estimate at −30 mV (see *Absolute Magnitude...*) so that effectively only four parameters are independent. For algebraic convenience, we chose to calculate K_{eq} from the others:

$$K_{eq} = \frac{1}{P_o\left[1 + e^{\frac{-z_\infty(V_\infty + 30)F}{RT}}\right]} - \left[1 + e^{\frac{z_a(V_a + 30)F}{RT}}\right]. \tag{14}$$

Eqs. 10 and 12 may be combined with our one-site (*1s*) model for open channel permeation (Eq. 6) to give an overall model, $p_a p_\infty$ *1s* (the product of Eqs. 6, 10, and 12), for the voltage dependence of steady-state TTX-sensitive current. Although fitting this model to normalized data (Fig. 10 A) discards information on absolute current magnitude, we used the mean value of TTX-sensitive currents measured under reference conditions, corrected for rundown, to recover the lost information (see *Absolute Magnitude...*).

Global Least-squares Fit to the Entire Data Set

We verified the ability of the $p_a p_\infty$ *1s* model, augmented with noncompetitive voltage-independent channel block by external NMG, to account for our combined findings on the following: (1) current ratios reflecting nonindependent permeation (Fig. 9 and similar experiments not shown); (2) the voltage dependence of steady-state TTX-sensitive inward and outward current (Fig. 10 A); and (3) inhibition by external NMG (Figs. 6 and 10 A). To this end, we fitted the model (using a single set of parameters) simultaneously to the entire data set. The augmented $p_a p_\infty$ *1s* model contains six independent parameters. Two (V_a and z_a) were taken from measurements of the steady-state voltage dependence of Na channel activation in squid giant axon (Vandenberg and Bezanilla, 1991). Our global fit then yields estimates (Table I) for the remaining four adjustable model parameters: $K_{Nai}(0)$, K_{NMG}, V_∞, and z_∞. K_{eq}, calculated via Eq. 14 from our estimate (0.0003; see next section) of P_o at −30 mV was 770, which is comparable to the corresponding value of $\kappa/\lambda = 1{,}000$ estimated for *L. pealei* by Bezanilla and Armstrong (1977). The principal determinants of the shape of the I-V curves in Fig. 10 A are the gating parameters (z_a, V_a, z_∞, and V_∞) that describe the voltage dependence of the channel's open probability in the steady state. The inversus outward current ratios (not only those obtained at −30 mV in Fig. 9 and similar experiments, but also those of the in- versus outward pairs at various voltages in Fig. 10 A) constrain the estimation of $K_{Nai}(0)$, the cause of nonindependent behavior. The NMG inhibition data in Fig. 6 and the 266/0 curve in Fig. 10 A yield K_{NMG} (the voltage-independent equilibrium constant for NMG block). All curves in Figs. 4 C, 6, and 10 are drawn using the parameters listed in Table I. A striking feature of Fig. 10 A is the fact that the outward currents do not steadily increase with voltage at positive membrane potentials, as would be expected (Fig. 10 A, dashed line) in a model lacking p_∞, the voltage-dependent inactivation factor. Also indicative of voltage-dependent inactivation is the inflection in the inward I-V curve near 0 mV.

Absolute Magnitude of the Persistent TTX-sensitive Current

After correction for rundown, we found the persistent TTX-sensitive current at −30 mV and 425 mM external [Na] to have an amplitude of 3.3 ± 0.3 μA cm^{-2} (11 axons). Baker et al. (1969) found a TTX-sensitive Na influx in resting intact *L. forbesi* axons in 10 mM K artificial seawater (and resting potential likely near −60 mV) of ~1.6 μA cm^{-2}, which is compatible with our results at −30 mV. To calculate the fraction of Na channels that remain open in the steady state requires knowledge of the current expected at −30 mV if all Na channels were open. Using the maximum Na conductance of 130 mS cm^{-2} for *L. pealei* axons at 20°C not exposed to internal fluoride (Rosenthal and Bezanilla, 2001; and Rosenthal, J.J.C., and F. Bezanilla, personal communication), we estimate the maximum possible inward Na current at −30 mV to be ~11 mA cm^{-2}, which implies that the persistently open fraction of the total population of channels at −30 mV averages only ~0.03% (i.e., $P_o = 0.0003$, the value we used to constrain the other fit parameters via Eq. 13). This is more than an order of magnitude smaller than the value of 0.43% predicted by the classical product $m^3(\infty)h(\infty)$, using the parameter values listed by Meves (1984). Even after introducing a slow inactivation factor, $s(\infty)$ (Rudy, 1978), the product $m^3(\infty)h(\infty)s(\infty)$ at −30 mV predicts a persistent open channel fraction of 0.19%, still much larger than our estimate. Fig. 10 B shows steady-state absolute open probabilities calculated for p_a alone as well as for the product $p_a p_\infty$, using the least-squares parameters found and the value calculated for K_{eq}. The latter defines the amplitude of the p_a curve asymptote at positive voltages. At −30 mV, the value of p_a (i.e., the steady-state open probability resulting solely from activation coupled to voltage-independent inactivation) is 0.0013. The voltage-dependent steady-state inactivation factor p_∞ of our model closes another 76% of those open channels, yielding the open probability of 0.0003 at −30 mV.

Assuming a Na-channel density in squid axon of ~600 μm^{-2} (Levinson and Meves, 1975) for a P_o of 0.0003 there will be 1.8×10^7 channels cm^{-2} open in the steady state at −30 mV, sustaining the observed zero-trans inward current of 3.3 μA cm^{-2} when $[Na]_o$ = 0.425 M, or 1.1×10^6 ions s^{-1} channel^{-1}. Eq. 8 then yields an estimate for the second-order rate coefficient $k_1(0) = \sim 2 \times 10^6$ s^{-1} M^{-1}. Any correction of the 130-mS cm^{-2} maximum Na conductance value for the inactivation likely present in those experiments would tend to increase our estimate of the maximum current at −30 mV (perhaps by about one third; Stimers et al., 1985). That would, in turn, further reduce (by the same factor) our estimate of the fraction of persistently open channels, engendering (via Eq. 13) minor adjustments in our fit parameters and estimate of $k_1(0)$.

Voltage-dependent Inactivation, or Block?

We do not know the mechanism underlying the voltage-dependent inactivation, but one possibility is block by internal Mg^{2+}, which is well documented for K channels (for review see Stanfield, 1988). Indeed, Pusch et al. (1989) have described voltage-dependent block of outward Na current by internal Mg^{2+} in *Xenopus* oocytes injected with cRNA encoding rat brain type II Na channels; $K_{0.5}$ at 0 mV was 3–4 mM. Since the free $[Mg^{2+}]$ in our experiments was ~12.5 mM (17.5 mM

TABLE I

Parameters Determined from the Overall Least-squares Fit

Description	Parameter	Units	Overall fit value
Open channel permeation:			
Equilibrium constant for internal Na^+ binding	$K_{Nai(0)}$	M	0.61 ± 0.08
Dissociation constant for external NMG block	K_{NMG}	mM	209 ± 15
Voltage-dependent inactivation (p_∞) gating parameters:			
Midpoint voltage of p_∞	V_∞	mV	−83 ± 5
Effective valance of p_∞	z_∞		0.55 ± 0.03
	Values calculated from those determined above		
Calculated value of the equilibrium constant for voltage-independent inactivation	K_{eq}		770
Alternative parameters calculated for internal Mg^{2+} block (p_{Mg}):			
Dissociation constant at 0 mV	$K_{Mg}(0)$	mM	2.0
Fractional depth of Mg^{2+} binding site from the inside	δ_{Mg}		0.28

total [Mg^{2+}] with 5 mM ATP present) we may consider a model of voltage-dependent Na-channel block by internal free Mg^{2+}, with the fraction of channels not blocked given by

$$p_{Mg} = \frac{1}{1 + \frac{[Mg^{2+}]}{K_{Mg}(0)} \cdot e^{\frac{\delta_{Mg} zVF}{RT}}}, \quad (15)$$

where $K_{Mg}(0)$ is the dissociation constant for the putative Mg^{2+} binding site at 0 mV, δ_{Mg} is the fraction of the membrane potential (V) at the site, and the valence of Mg^{2+} (z) is 2. Eq. 15 has the same canonical form as the empirical steady-state Eq. 12 we used to describe p_∞, steady-state voltage-dependent inactivation. The two formulations are identical when

$$V_\infty = \left(\frac{RT}{2F\delta_{Mg}}\right)\ln\left(\frac{K_{Mg}(0)}{[Mg^{2+}]}\right)$$

$$\text{and } z_\infty = 2\delta_{Mg}.$$

Substitution of Eq. 15 for Eq. 12, thus, yields an alternative model, $p_a p_{Mg}$ *1s*, indistinguishable from $p_a p_\infty$ *1s* until experiments are performed at various internal [Mg^{2+}]. The fit parameters obtained for this internal Mg^{2+} blocking model are also listed in Table I. With $K_{Mg}(0)$ = 2.0 mM and δ_{Mg} = 0.28, the "pure" Mg^{2+} block model yields the required 76% block at −30 mV.

Estimated K_d for TTX Binding to Persistent Na Channels

Cuervo and Adelman (1970), recording the time course of recovery of (depolarization induced) peak inward current after TTX withdrawal, found a mean time constant of 8.6 min at 7°C or (taking a Q_{10} of 2.0 calculated from their data) 4.3 min at 17°C, which compares reasonably with our value of 3.2 min (Fig. 2). Keynes et al. (1975) have pointed out that recovery of current does not straightforwardly reflect the rate of dissociation of bound TTX since the toxin's escape is retarded in the restricted-diffusion Frankenhaeuser-Hodgkin (Frankenhaeuser and Hodgkin, 1956) space within which it can rebind to vacant sites. After their treatment, the time constant, τ_{rec}, for the latter part of the recovery is $\tau_{rec} = N/(P_{TTX}K_d)$, where N is the surface concentration of TTX binding sites in moles per unit area, P_{TTX} is the apparent permeability to TTX of the virtual boundary delimiting the Frankenhaeuser-Hodgkin space, and K_d is the TTX dissociation constant. Assuming a site density of 600 μm^{-2} (Levinson and Meves, 1975) and a P_{TTX} value of 2×10^{-5} cm s^{-1} (Keynes et al., 1975), we calculate a K_d of 5 nM for TTX block of persistent Na-channel current, which is comparable to the value of 4.7 nM obtained by Schwarz et al. (1973) for peak Na current in frog myelinated nerve.

We thank Wolfgang Nonner for pointing out the work of Pusch et al. (1989).

This work was supported by National Institutes of Health grants NS-22979, HL-36783, and NS-11223.

Submitted: 13 September 2001
Revised: 18 January 2002
Accepted: 30 January 2002

REFERENCES

Adelman, W.J., and Y. Palti. 1969. The effects of external potassium and long duration voltage conditioning on the amplitude of sodium currents in the giant axon of the squid, *Loligo pealei*. *J. Gen. Physiol.* 54:589–606.

Almers, W., P.R. Stanfield, and W. Stühmer. 1983. Slow changes in currents through sodium channels in frog muscle membrane. *J. Physiol.* 339:253–271.

Baker, P.F., M.P. Blaustein, R.D. Keynes, J. Manil, T.I. Shaw, and R.A. Steinhardt. 1969. The ouabain-sensitive fluxes of sodium and potassium in squid giant axons. *J. Physiol.* 200:459–496.

Begenisich, T. 1987. Molecular properties of ion permeation through sodium channel. *Annu. Rev. Biophys. Biophys. Chem.* 16: 247–263.

Begenisich, T., and D. Busath. 1981. Sodium flux ratio in voltage-clamped squid giant axons. *J. Gen. Physiol.* 77:489–502.

Begenisich, T.B., and M.D. Cahalan. 1980a. Sodium channel permeation in squid axons I: reversal potential experiments. *J. Physiol.* 307:217–242.

Begenisich, T.B., and M.D. Cahalan. 1980b. Sodium channel permeation in squid axons II: non-independence and current-voltage relations. *J. Physiol.* 307:243–257.

Bezanilla, F., and C.M. Armstrong. 1977. Inactivation of the sodium channel: I. Sodium current experiments. *J. Gen. Physiol.* 70:549–566.

Chandler, W.K., and H. Meves. 1970. Evidence for two types of sodium conductance in axons perfused with sodium fluoride. *J. Physiol.* 211:653–678.

Correa, A., and F. Bezanilla. 1994a. Gating of the squid sodium channel at positive potentials. I. Macroscopic ionic and gating currents. *Biophys. J.* 66:1853–1863.

Correa, A., and F. Bezanilla. 1994b. Gating of the squid sodium channel at positive potentials. II. Single channels reveal two open states. *Biophys. J.* 66:1864–1878.

Crill, W.E. 1996. Persistent sodium current in mammalian central neurons. *Annu. Rev. Physiol.* 58:349–362.

Cuervo, L.A., and W.J. Adelman. 1970. Equilibrium and kinetic properties of the interaction between tetrodotoxin and the excitable membrane of the squid giant axon. *J. Gen. Physiol.* 55:309–335.

Cummins, T.R., and F.J. Sigworth. 1996. Impaired slow inactivation in mutant sodium channels. *Biophys. J.* 71:227–236.

Doyle, D.A., J. Morais Cabral, R.A. Pfuetzner, A. Kuo, J.M. Gulbis, S.L. Cohen, B.T. Chait, and R. MacKinnon. 1998. The structure of the potassium channel: molecular basis of K^+ conduction and selectivity. *Science.* 280:69–77.

Frankenhaeuser, B., and A.L. Hodgkin. 1956. The after-effects of impulses in the giant nerve fibres of *Loligo. J. Physiol.* 131:341–376.

Goldman, L., and C.L. Schauf. 1972. Inactivation of the sodium current in *Myxicola* giant axons. Evidence of coupling to the activation process. *J. Gen. Physiol.* 59:659–675.

Hille, B. 1975. Ionic selectivity, saturation and block in sodium channels: a four-barrier model. *J. Gen. Physiol.* 66:535–560.

Hille, B. 1992. Ionic Channels of Excitable Membranes, 2nd ed. Sinauer Associates, Inc., Sunderland, MA. 607 pp.

Hille, B., and W. Schwarz. 1978. Potassium channels as multi-ion single file pores. *J. Gen. Physiol.* 72:409–442.

Hodgkin, A.L., and A.F. Huxley. 1952a. The currents carried by sodium and potassium ions through the membrane of the giant axon of *Loligo. J. Physiol.* 116:449–472.

Hodgkin, A.L., and A.F. Huxley. 1952b. The dual effect of membrane potential on sodium conductance in the giant axon of *Loligo. J. Physiol.* 116:497–506.

Hodgkin, A.L., and A.F. Huxley. 1952c. A quantitative description of membrane current and its application to conduction and excitation in nerve. *J. Physiol.* 117:500–544.

Hodgkin, A.L., and R.D. Keynes. 1955. The potassium permeability of a giant nerve fibre. *J. Physiol.* 128:61–88.

Horn, R., J. Patlak, and C.F. Stevens. 1981. The effect of tetramethylammonium on single sodium channel currents. *Biophys. J.* 36: 321–327.

Keynes, R.D., F. Bezanilla, E. Rojas, and R.E. Taylor. 1975. The rate of action of tetrodotoxin on sodium conductance in the squid giant axon. *Phil. Trans. Roy. Soc. Lond. B.* 270:365–375.

Kirsch, G.E., and M.F. Anderson. 1986. Sodium channel kinetics in normal and denervated rabbit muscle membrane. *Muscle Nerve.* 10:738–747.

Levinson, S.R., and H. Meves. 1975. The binding of tritiated tetrodotoxin to squid giant axons. *Phil. Trans. Roy. Soc. Lond. B.* 270: 349–352.

Meves, H. 1984. Hodgkin-Huxley: Thirty years after. *Curr. Top. Membr. Transp.* 22:279–329.

Morais-Cabral, J.H., Y. Zhou, and R. MacKinnon. 2001. Energetic optimization of ion conduction rate by the K^+ selectivity filter. *Nature.* 414:37–42.

Levitt, D.G. 1999. Modeling of ion channels. *J. Gen. Physiol.* 113: 789–794.

Nonner, W., D.P. Chen, and B. Eisenberg. 1998. Anomalous mole fraction effect, electrostatics and binding in ionic channels. *Biophys. J.* 74:2327–2334.

Ohta, M., T. Narahashi, and R. Keeler. 1973. Effects of veratrum alkaloids on membrane potential and conductance of squid and crayfish giant axons. *J. Pharmacol. Exp. Ther.* 184:143–154.

Pusch, M., F. Conti, and W. Stühmer. 1989. Intracellular magnesium blocks sodium outward currents in a voltage- and dose-dependent manner. *Biophys. J.* 55:1267–1271.

Rakowski, R.F. 1989. Simultaneous measurement of changes in current and radiotracer flux in voltage-clamped squid giant axon. *Biophys. J.* 55:663–671.

Rakowski, R.F., D.C. Gadsby, and P. De Weer. 1989. Stoichiometry and voltage dependence of the sodium pump in voltage-clamped, internally-dialyzed squid giant axon. *J. Gen. Physiol.* 93: 903–941.

Rosenthal, J.J.C., and F. Bezanilla. 2001. Changes in Na^+ and K^+ conductance levels underlie species-dependent action potential properties in squid giant axon. *Biophys. J.* 80:209a. (Abstr.)

Ruben, P.C., J.G. Starkus, and M.D. Rayner. 1992. Steady state availability of sodium channels: interactions between activation and slow inactivation. *Biophys. J.* 61:941–955.

Rudy, B. 1978. Slow inactivation of the sodium conductance in squid giant axon: pronase resistance. *J. Physiol.* 283:1–21.

Schwarz, J.R., W. Ulbricht, and H.-H. Wagner. 1973. The rate of action of tetrodotoxin on myelinated nerve fibres of *Xenopus laevis* and *Rana esculenta. J. Physiol.* 233:167–194.

Simoncini, L., and W. Stühmer. 1987. Slow sodium channel inactivation in rat fast-twitch muscle. *J. Physiol.* 383:327–337.

Stanfield, P.R. 1988. Intracellular Mg^{2+} may act as a co-factor in ion channel function. *Trends Neurosci.* 11:475–477.

Stimers, J.R., F. Bezanilla, and R.E. Taylor. 1985. Sodium channel inactivation in the squid giant axon. Steady state properties. *J. Gen. Physiol.* 85:65–82.

Taylor, C.P. 1993. Na^+ currents that fail to inactivate. *Trends Neurosci.* 16:455–460.

Ussing, H.H. 1949. The distinction by means of tracers between active transport and diffusion. *Acta Physiol. Scand.* 19:43–56.

Vandenberg, C.A., and F. Bezanilla. 1991. Single-channel, macroscopic, and gating currents from sodium channels in the squid giant axon. *Biophys. J.* 60:1499–1510.